

Article

The Effect of Oxygen Tension on the Differentiation of Outgrowth Cells from Embryoid Bodies Produced by Mouse Induced Pluripotent Stem Cells

Hisashi Yano ^{1,*} , Takashi Inoue ², Satoshi Murakami ³ and Hiroyuki Kaneko ¹

¹ Department of Oral and Maxillofacial Surgery, Tokyo Women's Medical University Adachi Medical Center, Adachi, Tokyo 123-8558, Japan

² Tokyo College of Medical Technology, Sumida, Tokyo 130-0015, Japan

³ Department of Oral Pathology, Matsumoto Dental University, Nagano 399-0781, Japan

* Correspondence: yano.hisashi@twmu.ac.jp

Abstract: The purpose of this study was to investigate the effects of oxygen tension on mouse induced pluripotent stem (iPS) cells by assessing differentiation in terms of embryoid body (EB) size and mRNA and protein expression levels of collagen type 1 and Runx2. EBs and outgrowth cells (OGCs) were cultured in conditions of hypoxia (2%), normoxia (21%) and hyperoxia (35%). Significantly larger EBs were observed in the hyperoxia and normoxia groups compared to the hypoxia group on Days 8 and 10. The hyperoxia group had significantly higher mRNA and protein expression levels of collagen type 1 and Runx2 compared to the hypoxia and normoxia groups on Days 10 and 26, and these expression levels in the hypoxia group were significantly lower than the normoxia group on Days 10 and 26. These results suggest that hyperoxia accelerates the enlargement in EBs and the differentiation of iPS cells.

Keywords: cell differentiation; induced pluripotent stem cell; oxygen tension; embryoid bodies; outgrowth cells



Citation: Yano, H.; Inoue, T.; Murakami, S.; Kaneko, H. The Effect of Oxygen Tension on the Differentiation of Outgrowth Cells from Embryoid Bodies Produced by Mouse Induced Pluripotent Stem Cells. *Appl. Sci.* **2023**, *13*, 1215. <https://doi.org/10.3390/app13021215>

Academic Editors: Andrea Ballini, Michele Covelli, Antonio Boccaccio, Maria Contaldo and Dario Di Stasio

Received: 9 December 2022

Revised: 8 January 2023

Accepted: 11 January 2023

Published: 16 January 2023



Copyright: © 2023 by the authors. Licensee MDPI, Basel, Switzerland. This article is an open access article distributed under the terms and conditions of the Creative Commons Attribution (CC BY) license (<https://creativecommons.org/licenses/by/4.0/>).

1. Introduction

Induced pluripotent stem (iPS) cells were first established in 2006 by Takahashi and Yamanaka [1]. iPS cells were generated from mouse embryonic or adult fibroblasts after retrovirally introducing genes encoding four transcription factors (Oct3/4, Sox2, Klf4 and c-Myc). iPS cells are prime candidates for cell sources of cell regeneration therapy, because they retain their pluripotency. Two methods to differentiate iPS cells into target cells are known: embryoid body (EB)-mediated differentiation or direct differentiation of iPS cells. In this study, the EB-mediated differentiation method was used. Outgrowth cells (OGCs) from EBs can be used to differentiate further them into other types of cells. Several studies have reported that cell differentiation is influenced by a variety of physicochemical factors, such as matrix composition and mechanical stress.

Oxygen tension is also known to be an important factor for iPS cell differentiation. The in situ oxygen tension is considerably lower than atmosphere levels. Thus, many studies on cell differentiation under hypoxia conditions have been reported, but little is known about the effects of high oxygen tension for the differentiation of cells. On the other hand, hyperbaric oxygen therapy is an effective treatment for severe bone fractures, and it promotes quick and complete healing of bones. However, few studies have focused on the effects of higher oxygen tension on the formation of EBs from iPS cells and iPS cell differentiation.

Osteo-differentiation is a process that happens gradually. Several specific markers can be examined to determine the differentiation state of the cells [2]. Runt-related transcription factor 2 (Runx2) is an early osteo-differentiation marker that is critical for the

osteo-differentiation process [3]. Runx2 regulates the differentiation of mesenchymal progenitor cells into pre-osteoblasts. These bone progenitor cells initiate the production of collagen type 1, the most abundant type of collagen in the body [4]. Collagen type 1 is the principal organic component of the bone extracellular matrix. Lynch et al. [5] suggested that collagen type 1 is involved in mediating the signaling cascade associated with enhancing the expression of the differentiated phenotype of osteoblasts and accelerating the mineralization of the matrix *in vitro*. Forming EBs followed by harvesting OGCs and differentiating them into the osteogenic lineage requires the expression of type 1 collagen and Runx2 [2].

The aim of this study was to investigate the effects of oxygen tension (hyperoxia, normoxia and hypoxia) on the size of EBs and on iPS cell differentiation in terms of the expression of collagen type 1 and Runx2, which are markers of early osteogenesis.

2. Materials and Methods

2.1. Cell Culture

Mouse iPS cells (miPSCs) that produce green fluorescent protein (GFP) regulated by the Nanog promoter were provided by the Riken Cell Bank (cell No. ASP0001, cell name iPS-MEF-Ng-20D-17) and were cultured as previously reported [6]. miPSCs were maintained on SNL 76/7 feeder cells and created cell colonies in iPS medium consisting of high glucose DMEM (Nacalai Tesque, Kyoto, Japan), 15% knockout serum replacement (KSR) (Gibco, Grand Island, NY, USA), 10 mM nonessential amino acids (Gibco, Grand Island, NY, USA), 200 mM L-glutamine (Gibco, Grand Island, NY, USA), 55 mM 2-mercaptoethanol (Gibco, Grand Island, NY, USA) and 10 µg/mL murine leukemia inhibitory factor (Wako, Osaka, Japan) for three passages. Colonies were then dissociated using Accutase® (Millipore, Temecula, CA, USA) into single cells and were switched to feederless cell cultures using ESGRO® Complete Plus Serum Free Clonal Grade Medium and ESGRO® Basal Medium (Millipore, Temecula, CA, USA), according to the manufacturer's instructions, and were then cultured for five passages before being used in these experiments. Cell cultures for the above procedures were kept in a tissue culture incubator at 37 °C, 5% CO₂ and 21% O₂.

2.2. Experimental Design

The formation of EBs and OGCs at various oxygen tensions was characterized (Figure 1). EBs were classified into two categories according to the stage of differentiation: simple EBs and cystic EBs [7–9]. When ES cells were cultured in suspension for 2 to 4 days, spherical ES cell aggregates were formed. These ES cell aggregates with morula-like structures were called simple EBs. After 4–5 days of continuous suspension, a cavity was formed in the center of each EB. This stage of EBs was called cystic EBs. Cystic EBs resemble follicular embryos or embryos at the egg cylinder stage, with a double-layered structure surrounding the cavity. After 8 to 10 days in suspension culture, the cystic EBs expanded into large cystic structures resembling the internal yolk sac of a post-implantation embryo. Kurosawa et al. [10] suggested that these large cystic EBs correspond to the late stage and should be differentiated from EBs up to day 5. Therefore, we decided to change the oxygen concentration from day 5, corresponding to the late stage of EBs, referring to the differentiation process of actual fertilized eggs. In order to form EBs in this study, we performed the modifications detailed by Nakatsuji and Suemori [11]. Briefly, miPSC cell colonies were dissociated using 0.25% trypsin-EDTA (Gibco, Grand Island, NY, USA) into single cells that were resuspended in EB formation medium consisting of high glucose DMEM, 10% fetal bovine serum (FBS) (Biosera, Nuaille, France) and 10% KSR. Cells were used at a concentration of 3000 cells per 20 µL to form EBs using the hanging drop method for 48 h at 37 °C, 5% CO₂ and 21% O₂. This day is considered Day 0 of the study. Subsequently, EBs were transferred to low-attachment bacterial culture dishes in EB formation medium and were grown as suspension cultures for 72 h at 37 °C, 5% CO₂ and 21% O₂. Our preliminary study found that the undifferentiated characteristics of EBs remained until Day 5 (unpublished data). The EBs were then divided into three oxygen

tension groups on Day 5, a hypoxia group (2% O₂), a normoxia group (21% O₂) and a hyperoxia group (35% O₂). The oxygen levels in cell cultures were controlled using a multi gas incubator (SMA-30; Astec, Fukuoka, Japan). Five days after the change to each of the oxygen tensions, i.e., on Day 10 from the EB formation, 20 EBs were seeded in gelatin-coated 35 mm cell culture dishes to allow the formation of OGCs, and the medium was switched to MEM Alpha (Gibco, Grand Island, NY, USA) with 10% FBS. Cells were then maintained until 16 days after the change of oxygen tension, i.e., Day 26 from the EB formation, with medium changes every 2 days. EBs and OGCs were evaluated on Days 10 and 26, respectively, using qRT-PCR and immunocytofluorescence (ICF) staining.

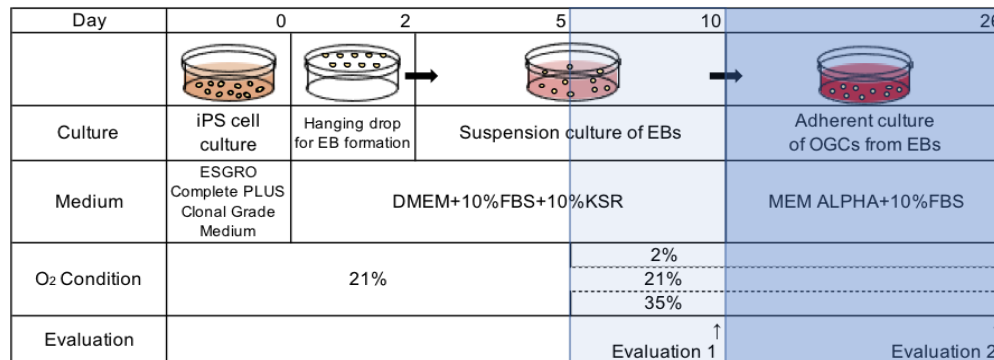


Figure 1. Scheme of the experimental design. Day 0 is the first day of the hanging drop method for EB formation. Day 2 is the first day of suspension culture for EBs. Shaded areas show the experimental design. Five days after the suspension for EB formation, different oxygen tensions were examined. The EBs at Day 10 were evaluated in terms of size, expression of mRNA and protein (arrow 1), after which the EBs were put in 35 mm dishes for OGC formation. Sixteen days (26 days in total days) after the adherent culture, OGCs were evaluated in terms of their expression of mRNA and protein (arrow 2).

2.3. Observation of EB Formation

The formation of EBs was observed and their sizes in μm were measured in micrographs (mean value \pm standard error) on Days 2, 5, 8 and 10. Specimens were observed and photographed using a BZ-X710 fluorescence phase contrast microscope (KEYENCE, Osaka, Japan). Expression of the Nanog promoter in iPS cells was observed using a fluorescent microscope by confirming the emission of light by GFP.

2.4. Quantitative Real-Time PCR Analysis

Total RNAs were extracted using a RNeasy[®] Mini Kit (QIAGEN, Hilden, Germany) according to the manufacturer's instructions. Each total RNA was reverse-transcribed and amplified using ReverTra Ace[®] qPCR RT Master Mix with gDNA Remover (Toyobo, Osaka, Japan) and cDNAs were synthesized. Quantitative RT-PCR was performed using TaqMan Gene Expression Assays (Applied Biosystems, Life Technologies, Carlsbad, CA, USA) for three target genes: collagen type I α 1 (collagen type 1), which was detected as a bone matrix marker, runt-related transcription factor 2 (Runx2), which was detected as a marker of osteoblasts and glyceraldehyde phosphate dehydrogenase (GAPDH), which is used as an endogenous control; primers used are shown in Table 1. A real-time PCR 7500 fast system (Applied Biosystems, Carlsbad, CA, USA) was used, and the relative expression of each target gene was estimated using the $\Delta\Delta\text{Ct}$ method.

Table 1. qRT-PCR Primers Used in this Study.

Primer	Gene Name	Assay ID
Collagen Type I	Collagen type I alpha 1	Mm00801666_g1
Runx2	Runt-related transcription factor 2	Mm00501580_m1
GAPDH	Glyceraldehyde-3-phosphate dehydrogenase	Mm99999915_g1

2.5. Immunocytofluorescence (ICF) Staining

On Days 10 and 26, EBs and OGCs were fixed in 4% paraformaldehyde for 15 min at 4 °C, and then were permeabilized by 0.1% Triton X-100 in PBS for 15 min. EBs and OGCs were blocked with 10% goat serum for 1 h at room temperature and were then incubated overnight at 4 °C with primary antibodies to collagen type 1 (1:500, ab34710, Abcam, Cambridge, UK) and Runx2 (1:100, ab76956, Abcam, Cambridge, UK). Each sample was then washed with PBS and incubated with a secondary antibody conjugated to Alexa fluor[®] 488 (1:200, Invitrogen, Carlsbad, CA, USA) for 30 min at room temperature. The samples were mounted using ProLong[™] Diamond Antifade Mountant with DAPI (Life Technologies, Carlsbad, CA, USA) for nuclear counter staining.

2.6. Evaluation of the Intensity of Fluorescence in ICF Images

Each group of specimens was observed and photographed using a LSM 880 NLO (Carl Zeiss Microscopy GmbH, Jena, Germany) confocal laser scanning microscope. Quantitation of the intensity of fluorescence ICF images was performed using Fiji/ImageJ2 software (<https://fiji.sc>, accessed on 26 April 2021) [12].

2.7. Statistical Analysis

The experimental results were compared for variance using Bartlett's test. The results were analyzed via one-way ANOVA and were then compared by Tukey's test when no significant difference was found (p -value > 0.05). When comparison of variances using Bartlett's test revealed a significant difference (p -value < 0.05), data were analyzed using the Steel–Dwass test. A p -value < 0.05 is considered statistically significant for all analyses, using JMP pro Statistical software (version 14.0.0; SAS Institute, Cary, NC, USA).

3. Results

3.1. Evaluation of EBs

On Days 2 and 5, the expression of Nanog was observed in almost the entire area of each EB (Figure 2a,b), but the expression of Nanog was clearly attenuated in EBs cultured under normal oxygen conditions on Days 8 or 10 (Figure 2d,g). The size of EBs on Day 2, equivalent to the point in time when the hanging drop method was finished, was $318.65 \pm 3.44 \mu\text{m}$ (N = 20, range 295 to 368 μm) (Figure 3) and by Day 5 it had increased to $519.80 \pm 18.44 \mu\text{m}$ (N = 20, range 362 to 704 μm). The size of EBs on Day 8 in the hypoxia group was $635.05 \pm 19.25 \mu\text{m}$ (N = 37, range 503 to 837 μm), in the normoxia group it was $740.83 \pm 22.89 \mu\text{m}$ (N = 115, range 413 to 1234 μm) and in the hyperoxia group it was $744.37 \pm 12.74 \mu\text{m}$ (N = 49, range 444 to 1205 μm). EBs in the normoxia and hyperoxia groups were significantly larger on Day 8 compared with EBs in the hypoxia group, but there was no significant difference between the normoxia and the hyperoxia groups. The size of EBs on Day 10 in the hypoxia group was $637.43 \pm 26.91 \mu\text{m}$ (N = 56, range 529 to 888 μm), in the normoxia group it was $943.16 \pm 41.52 \mu\text{m}$ (N = 92, range 532 to 1692 μm) and in the hyperoxia group it was $945.67 \pm 10.27 \mu\text{m}$ (N = 51, range 611 to 1956 μm). EBs in the normoxia and the hyperoxia groups were significantly larger compared to EBs in the hypoxia group on Day 10, and, as was the case on Day 8, there was no significant difference between EBs in the hyperoxia and normoxia groups. EBs in the hyperoxia group had a significantly larger size than EBs in the hypoxia group, and the standard errors tended to be smaller. The size of EBs became larger from Days 2 to 5. The size of EBs in the normoxia and hyperoxia groups became larger from Day 5 to Day 10. The size of EBs in the hypoxia

group on Day 8 became larger compared to Day 5 but was smaller than EBs in the other two groups, and was about the same size on Days 8 and 10, meaning that they had not increased in size.

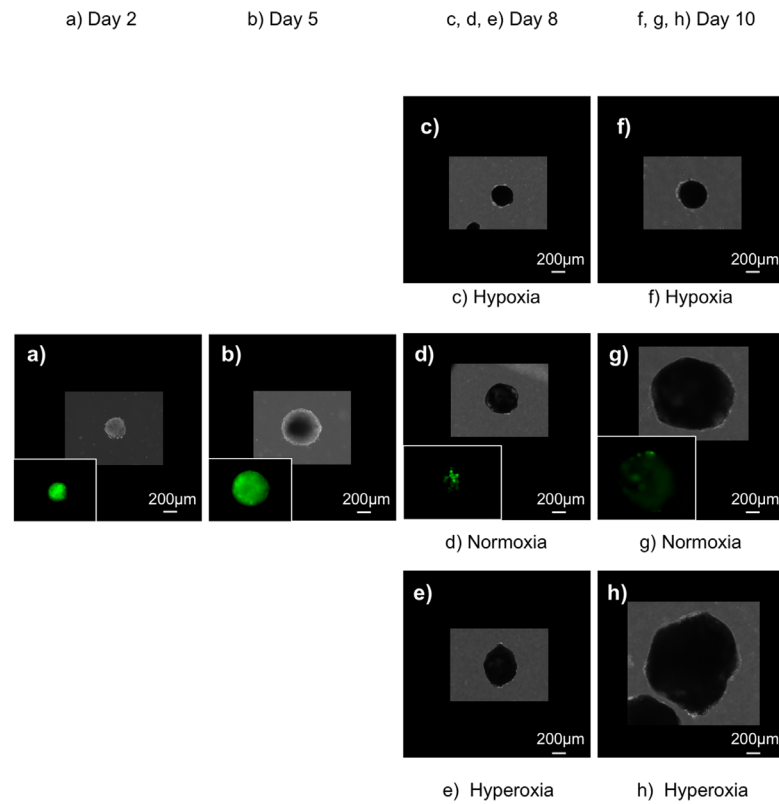


Figure 2. Phase contrast and fluorescence microscopy of EBs on Days 2, 5, 8 and 10. Note the change in size of EBs and the pattern of Nanog expression (green).

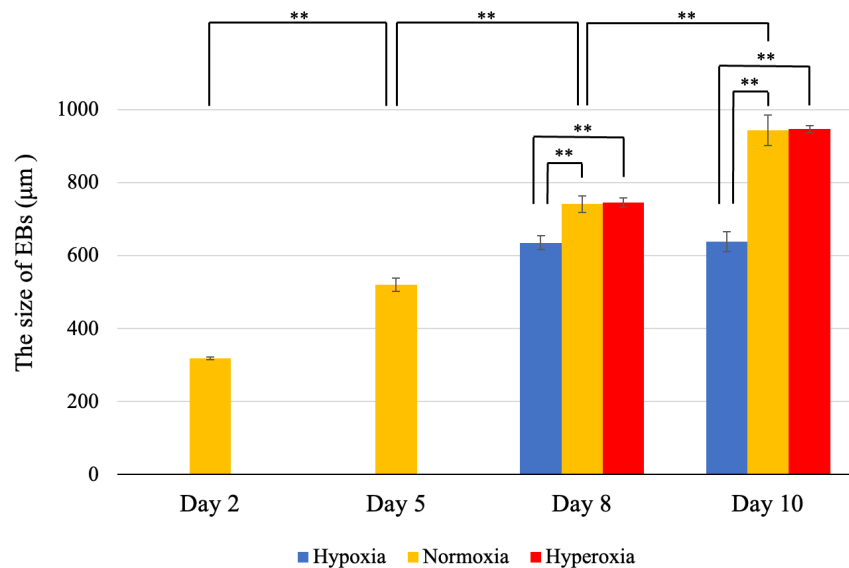


Figure 3. Transition of EB size. EB size was measured using a phase contrast microscope, and the transition of EB size was evaluated. Two asterisks (**) indicate that the *p*-value < 0.01.

3.2. qRT-PCR Analysis of Gene Expression Patterns

On Day 10, the mRNA expression level of collagen type 1 was significantly higher in the hyperoxia group (N = 6) than in the normoxia group (N = 12), and the levels in both those

groups were significantly higher than the hypoxia group (N = 6) (Figure 4a). The differences in collagen type 1 mRNA expression levels among these three groups were statistically significant. At Day 10, the mRNA expression level of Runx2 was significantly higher in the hyperoxia group than in both the normoxia and hypoxia groups (Figure 4b). The differences in Runx2 mRNA expression levels among these three groups were statistically significant. The hyperoxia group had the highest and the hypoxia group had the lowest mRNA expression levels for both collagen type 1 and Runx2.

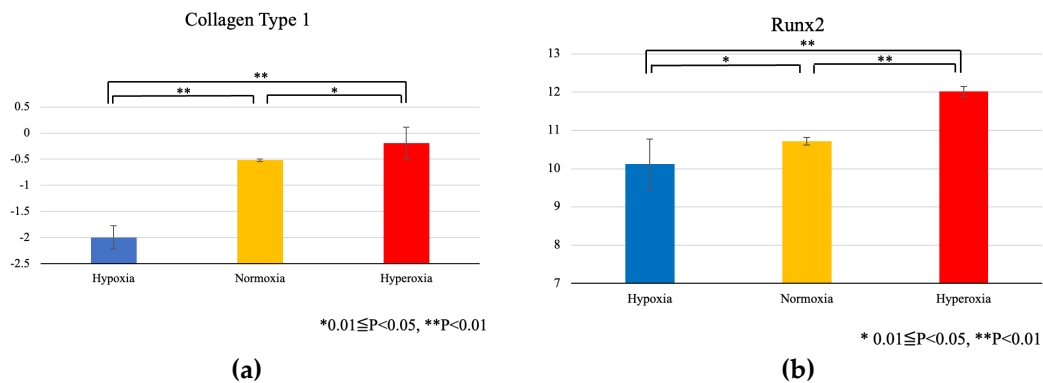


Figure 4. Collagen type 1 (a) and Runx2 (b) mRNA expression levels in EBs on Day 10. One asterisk (*) indicates that $0.01 \leq p\text{-value} < 0.05$. Two asterisks (**) indicate that the $p\text{-value} < 0.01$.

3.3. ICF Staining for Collagen Type 1 and Runx2 Proteins

Staining for collagen type 1 and Runx2 proteins was positive (green) in the EBs from all three groups (n = 6 for all three groups). The staining of collagen type 1 in the hyperoxia group showed a higher expression level compared with the other two groups (Figure 5a–c). Furthermore, Runx2 staining in EBs of the hyperoxia group was more highly expressed compared to other two groups (Figure 5d–f).

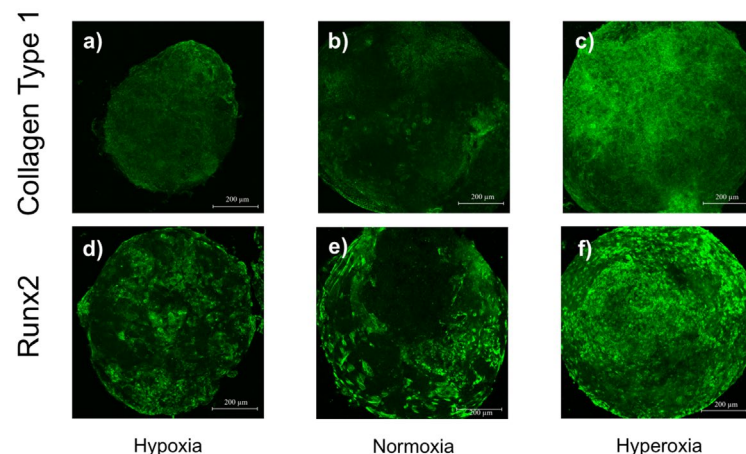


Figure 5. ICF staining for collagen type 1 (a–c) and Runx2 (d–f) proteins in EBs on Day 10.

3.4. Intensity of Fluorescence in ICF Staining Images

In ICF staining for collagen type 1 and Runx2 protein expression, EBs of the hyperoxia group showed the highest intensity compared with the other two groups (Figure 6 a,b). The hypoxia group had the lowest intensity and the differences were statistically significant in all three groups (n = 9 for all three groups).

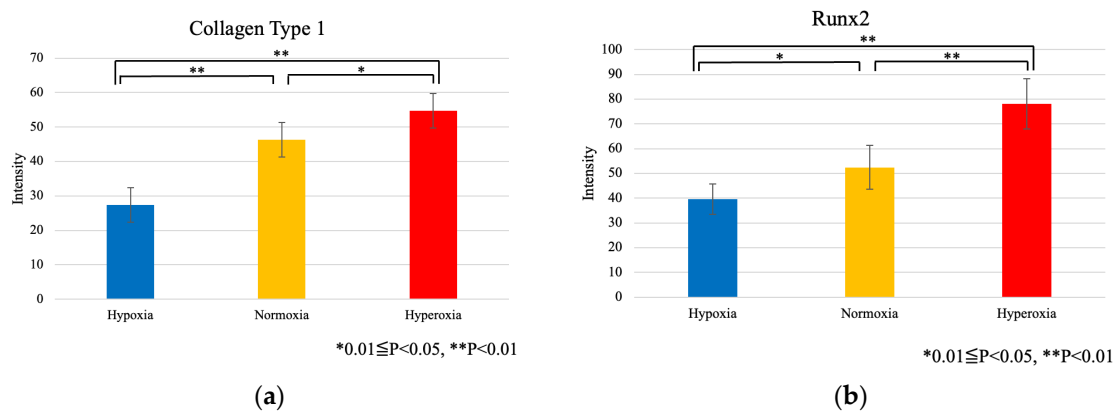


Figure 6. Comparison of the intensity of fluorescence in ICF staining for collagen type 1 (a) and Runx2 (b) expression levels in EBs on Day 10. One asterisk (*) indicates that $0.01 \leq p\text{-value} < 0.05$. Two asterisks (**) indicate that the $p\text{-value} < 0.01$.

3.5. Evaluation of OGCs

3.5.1. qRT-PCR Analysis of mRNA Expression Levels

On Day 26, the mRNA expression level of collagen type 1 in OGCs was significantly higher in the hyperoxia group (N = 6) than in the normoxia (N = 12) and hypoxia groups (N = 6) (Figure 7a). The mRNA expression level of collagen type 1 in OGCs in the hypoxia group was lower than in the normoxia group but the difference was not significant. On Day 26, the mRNA expression level of Runx2 was significantly higher in the hyperoxia group than in the normoxia and hypoxia groups (Figure 7b). Moreover, the expression level of Runx2 mRNA in the normoxia group was significantly higher than in the hypoxia group. The mRNA expression level of collagen type 1 was higher on Day 26 than on Day 10 in all three groups, and the mRNA expression levels of Runx2 showed the same tendencies as collagen type 1 mRNA.

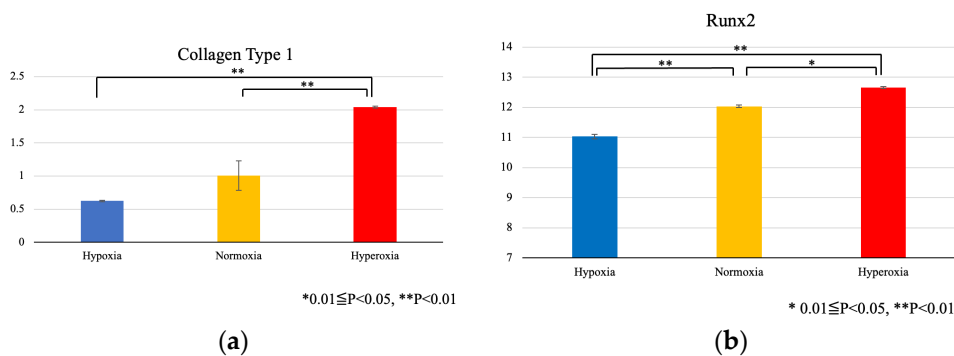


Figure 7. Collagen type 1 (a) and Runx2 (b) mRNA expression levels on Day 26 in OGCs. One asterisk (*) indicates that $0.01 \leq p\text{-value} < 0.05$. Two asterisks (**) indicate that the $p\text{-value} < 0.01$.

3.5.2. ICF Staining of Collagen Type 1 and Runx 2 Proteins

The ICF staining behavior of OGCs was similar to the EB behavior as described above. Collagen type 1 positive OGCs in the hyperoxia group were more strongly stained and a wider area was positive on comparison to the hypoxia group (Figure 8a–c). Runx2 staining was seen in the cytoplasm and nuclei of OGCs (Figure 8d–f). In the hyperoxia group, many Runx2 positive OGCs were observed, much more so than in the normoxia and hypoxia groups. However, only a few differences were seen (n = 6, for all three groups).

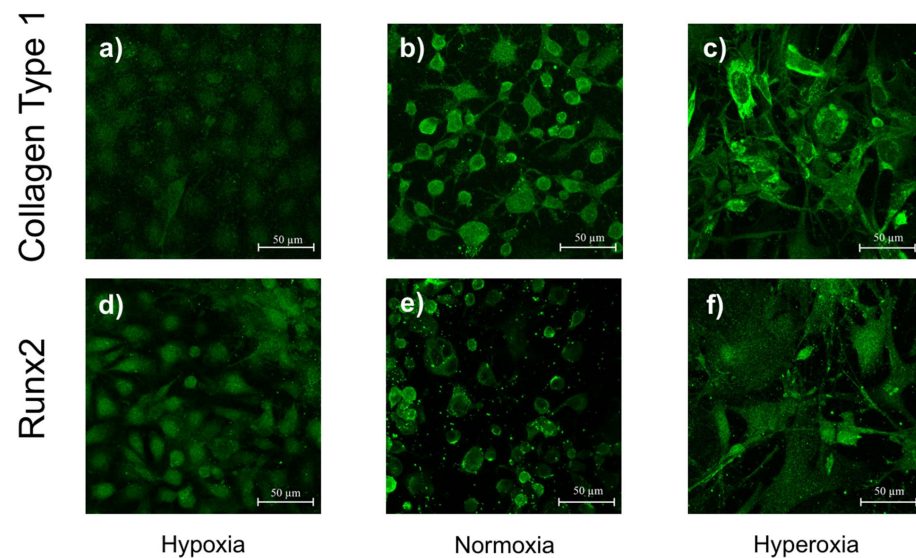


Figure 8. ICF staining for collagen type 1 (a–c) and Runx2 (d–f) proteins in OGCs on Day 26.

3.5.3. Intensity of Fluorescence in ICF Staining Images of OGCs

In ICF staining for collagen type 1 protein, OGCs of the hyperoxia group (N = 419) showed the highest intensity on Day 26, and OGCs of the hypoxia group (N = 1660) showed the lowest intensity (Figure 9a,b). ICF staining of Runx2 protein in OGCs of the hyperoxia group was significantly higher than the other two groups, and showed the same tendency as collagen type 1. These results were consistent with the results of qRT-PCR analysis (OGCs of the normoxia group: N = 1561).

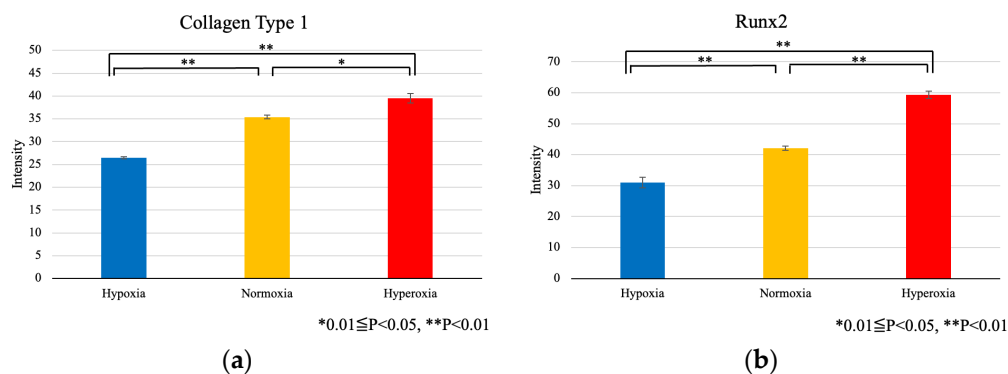


Figure 9. Comparison of the intensity of fluorescence in ICF staining for collagen type 1 (a) and Runx2 (b) proteins on Day 26. One asterisk (*) indicates that $0.01 \leq p\text{-value} < 0.05$. Two asterisks (**) indicate that the $p\text{-value} < 0.01$.

4. Discussion

The oxygen tensions used in this study define hypoxia as 2% O₂, normoxia as 21% O₂ and hyperoxia as 35% O₂. The reasons for these oxygen tension settings were that most previous studies that increased the differentiation of cells in hypoxia were set at 10% O₂ or less, and 2% O₂ was particularly effective [13–16]. On the other hand, many studies have reported the effects of hyperoxia at 35% O₂ [17–20]. Shaw and Basset reported that the highest level of ossification was observed at 35% O₂ [17], and therefore hyperoxia was defined as 35% O₂ in this study.

4.1. Decrease of Nanog Expression and Increase of EB Size Depend on Oxygen Tension

The size of EBs increased over time from Day 2 to Day 10. Nanog, which is an index of the undifferentiated state, was expressed on Days 2 and 5 but was not expressed on

Days 8 or 10, indicating that the undifferentiated characteristics of EBs were kept until Day 5. The results of this study supported the speculation of Kurosawa et al. [10], that the differentiation state of EBs differs before and after Day 5.

The oxygen tension was changed on Day 5 in this study because the increases in EB size were insufficient on Day 2, and the state of differentiation of EBs had progressed by Day 10. As a result, the size of EBs cultured under hypoxia remained smaller than the size of EBs cultured under normoxia, and EBs grew even larger under hyperoxia. According to Gassmann et al., when EBs were formed from mouse embryonic stem (ES) cells and were cultured under hypoxia (1%) for 5 days, they were found to grow equally [21]. However, the number of viable EBs decreased when the culture was continued for 5 days. That study did not comment on the size of the EBs, but the results suggested that hypoxia suppressed the increased number of cells constituting EBs. In addition, according to a study by Iida et al., hypoxia (3%) at the initial stage of the re-programming strengthened the colonization when hiPS cells were produced from dental pulp cells [22]. However, hypoxia strongly inhibited the colonization and the increase in hiPS cells at a late stage. Furthermore, according to Kurosawa et al., when mouse ES cells were cultured under hypoxia (5%), normoxia (20%) or hyperoxia (40%) for 4 days, cells proliferated the most in hyperoxia and the least in hypoxia [23]. In this study, we changed the oxygen tension to hypoxia on Day 5 of EB formation. As a result, the increase in EBs was suppressed; thus, our results confirmed the above results. Cell death can result easily due to a lack of oxygen and nourishment within cell agglomerations, which suggests that this was why the proliferative rate decreased [24]. Hypoxia decreased the number of mitochondria in cells, and it was thought that a metabolism change, such as the citric acid cycle [25], might have influenced that. However, one study reported that no difference was seen in the proliferative rate of cells with hypoxia (2%) or normoxia in periodontal ligament stem cells or in dental pulp stem cells [26]. In addition, there was a report that hypoxia (5%) enhanced the generation of iPS cells [27]. In other words, these findings suggest that many factors may play important roles in regulating the proliferation and differentiation of iPS cells, such as the type of cell, the oxygen tension, the exposure state and the time. On the other hand, hyperoxia increased the size of EBs and the quantity of OGCs in this study. It has been reported that an increase in oxygen tension allows Wnt signal transmission to regulate an increase in differentiation and cell activation [28].

4.2. Effects of Oxygen Tension on the Expression of Collagen Type 1 and Runx2 by iPS Cells

The mRNA expression level of collagen type 1 in EBs on Day 10 was significantly suppressed in the hypoxia group compared with the normoxia group, and was significantly stimulated in the hyperoxia group. The mRNA expression level of Runx2 in EBs on Day 10 showed a similar tendency to the expression of collagen type 1 mRNA on Day 10. These results suggest that EB differentiation under a hypoxia environment was suppressed. The mRNA expression levels of collagen type 1 and Runx2 in OGCs on Day 26 showed a similar result, and the differentiation of OGCs from EBs was more aggravated. In addition, hyperoxia promoted an increase in EBs.

Hypoxia conditions (2% O₂) decreased the expression of Runx2 in MG63 cells, which are human osteoblast-like cells [13]. Tuncay et al. reported that when osteoblast-enriched cultures from fetal rat calvariae were exposed to hyperoxia (90% O₂) or hypoxia (10% O₂), the levels of alkaline phosphatase and collagen were decreased in the hypoxia environment and the differentiation of osteoblasts was suppressed [14]. In addition, hypoxia conditions (3% O₂) have been shown to regulate the osteoplast differentiation of mouse ES cells [29]. It was reported that the hypoxia state reinforces the pluripotency of iPS cells [30–32]. Furthermore, hypoxia inducible factor (HIF) is expressed when iPS cells are exposed to a hypoxia environment, and contributes to the control of stemness by transcription network under hypoxia conditions [15]. The expression of HIF-1 α plays an important role in regulating the maturation of bone cells and calcification [33]. Hypoxia conditions promote cartilage differentiation from MSCs [34].

The classification of pluripotent stem cells into naive and primed populations was introduced some time ago [35]. The naive population is equivalent to a preimplantation blast cyst, and the primed population is equivalent to an embryo after implantation [36]. Mouse ES/iPS cells were classified as a naïve population. Glycolytic pathway metabolism is important to maintain pluripotency, but naive cells use oxidative phosphorylation [27,37,38]. Suppression of the glycolytic pathway and activation of oxidative phosphorylation were caused by a differentiation experiment of ES/iPS cells without determination of differentiation [32,39]. The shift to a similar metabolic pathway is probably caused by hyperoxia conditions. For this reason, it is thought that hyperoxia conditions alter metabolism and promote differentiation.

There are clear differences between the characteristics of miPS cells and hiPS cells derived under standard conditions [40]. Since mouse iPS cells were used in this experiment, these results cannot be directly applied to human iPS cells. However, since both mouse and human iPS cells have similar properties, such as enhanced pluripotency under the state of hypoxia state [30–32], it is possible that the same results as in this experiment can be expected for hiPS cells.

5. Conclusions

Hyperoxia promotes the differentiation of EBs and OGCs produced by mouse iPS cells in terms of early stage of osteogenesis.

Author Contributions: H.Y., T.I., S.M., H.K. contributed to conceptualization, methodology, validation, formal analysis, investigation, writing—original draft preparation and writing—review and editing. All the authors have read and agreed to the final version of the manuscript. All authors have read and agreed to the published version of the manuscript.

Funding: This research was supported in part by the Grant-in-Aid for Scientific Research from the Japan Society for the Promotion of Science (No.19K10118).

Institutional Review Board Statement: Not applicable.

Informed Consent Statement: Not applicable.

Data Availability Statement: Data sharing is not applicable.

Acknowledgments: We express our great appreciation to Akram Al-Wahabi and Tungalag Ser-Od whose comments and suggestions were of inestimable value for this study.

Conflicts of Interest: The authors declare no conflict of interest.

References

1. Takahashi, K.; Yamanaka, S. Induction of Pluripotent Stem Cells from Mouse Embryonic and Adult Fibroblast Cultures by Defined Factors. *Cell* **2006**, *126*, 663–676. [[CrossRef](#)]
2. Al Wahabi, A.; Ser Od, T.; Inoue, K.; Nakajima, K.; Matsuzaka, K.; Inoue, T. Topography Enhances Runx2 Expression in Outgrowing Cells from IPS Cell-Derived Embryoid Bodies. *J. Biomed. Mater. Res. B Appl. Biomater.* **2019**, *107*, 2288–2296. [[CrossRef](#)]
3. James, A.W. Review of Signaling Pathways Governing MSC Osteogenic and Adipogenic Differentiation. *Scientifica* **2013**, *2013*, 684736. [[CrossRef](#)]
4. Liu, Y.; Goldberg, A.J.; Dennis, J.E.; Gronowicz, G.A.; Kuhn, L.T. One-Step Derivation of Mesenchymal Stem Cell (MSC)-like Cells from Human Pluripotent Stem Cells on a Fibrillar Collagen Coating. *PLoS ONE* **2012**, *7*, e33225. [[CrossRef](#)]
5. Lynch, M.P.; Stein, J.L.; Stein, G.S.; Lian, J.B. The Influence of Type I Collagen on the Development and Maintenance of the Osteoblast Phenotype in Primary and Passaged Rat Calvarial Osteoblasts: Modification of Expression of Genes Supporting Cell Growth, Adhesion, and Extracellular Matrix Mineralization. *Exp. Cell Res.* **1995**, *216*, 35–45. [[CrossRef](#)]
6. Egusa, H.; Kayashima, H.; Miura, J.; Uruguchi, S.; Wang, F.F.; Okawa, H.; Sasaki, J.I.; Saeki, M.; Matsumoto, T.; Yatani, H. Comparative Analysis of Mouse-Induced Pluripotent Stem Cells and Mesenchymal Stem Cells During Osteogenic Differentiation In Vitro. *Stem Cells Dev.* **2014**, *23*, 2156–2169. [[CrossRef](#)]
7. Abe, K.; Niwa, H.; Iwase, K.; Takiguchi, M.; Mori, M.; Abé, S.I.; Abe, K.; Yamamura, K.I. Endoderm-Specific Gene Expression in Embryonic Stem Cells Differentiated to Embryoid Bodies. *Exp. Cell Res.* **1996**, *229*, 27–34. [[CrossRef](#)]
8. Magyar, J.P.; Nemir, M.; Ehler, E.; Suter, N.; Perriard, J.C.; Eppenberger, H.M. Mass Production of Embryoid Bodies in Microbeads. *Ann. N. Y. Acad. Sci.* **2001**, *944*, 135–143. [[CrossRef](#)]

9. Conley, B.J.; Young, J.C.; Trounson, A.O.; Mollard, R. Derivation, Propagation and Differentiation of Human Embryonic Stem Cells. *Int. J. Biochem. Cell Biol.* **2004**, *36*, 555–567. [CrossRef]
10. Kurosawa, H. Methods for Inducing Embryoid Body Formation: In Vitro Differentiation System of Embryonic Stem Cells. *J. Biosci. Bioeng.* **2007**, *103*, 389–398. [CrossRef]
11. Nakatsuji, N.; Suemori, H. *ES IPS Cell Experiments Standard Protocols*; Yodosha: Tokyo, Japan, 2014; pp. 246–257. ISBN 978-4-7581-0189-9.
12. Schindelin, J.; Arganda-Carreras, I.; Frise, E.; Kaynig, V.; Longair, M.; Pietzsch, T.; Preibisch, S.; Rueden, C.; Saalfeld, S.; Schmid, B.; et al. Fiji: An Open-Source Platform for Biological-Image Analysis. *Nat. Methods* **2012**, *9*, 676–682. [CrossRef]
13. Park, J.H.; Park, B.H.; Kim, H.K.; Park, T.S.; Baek, H.S. Hypoxia Decreases Runx2/Cbfa1 Expression in Human Osteoblast-like Cells. *Mol. Cell. Endocrinol.* **2002**, *192*, 197–203. [CrossRef]
14. Tuncay, O.C.; Ho, D.; Barker, M.K. Oxygen Tension Regulates Osteoblast Function. *Am. J. Orthod. Dentofac. Orthop.* **1994**, *105*, 457–463. [CrossRef]
15. Bertout, J.A.; Patel, S.A.; Simon, M.C. Hypoxia and Metabolism Series—Timeline the Impact of O-2 Availability on Human Cancer. *Nat. Rev. Cancer* **2008**, *8*, 967–975. [CrossRef]
16. Bassett, C.A.L. Current Concepts of Bone Formation. *J. Bone Jt. Surg.* **1962**, *44*, 1217–1244. [CrossRef]
17. Shaw, J.L.; Bassett, C.A.L. The Effects of Varying Oxygen Concentrations on Osteogenesis and Embryonic Cartilage in Vitro. *J. Bone Jt. Surg.* **1967**, *49*, 73–80. [CrossRef]
18. Wright, J.; Hyperbaric Oxygen Therapy for Wound Healing. *World Wide Wounds* 2001. Available online: <http://www.worldwidewounds.com/2001/april/Wright/HyperbaricOxygen.html>. (accessed on 6 November 2022).
19. Corcoran, T.; Ting, S.; Mas, E.; Phillips, M.; O’Loughlin, E.; Barden, A.; Mori, T.A. Hyperbaric Oxygen Therapy Is Not Associated with Oxidative Stress Assessed Using Plasma F-2-Isoprostanes and Isofurans. *Prostaglandins Leukot. Essent. Fat. Acids* **2017**, *127*, 16–19. [CrossRef]
20. Kemmler, J.; Bindl, R.; McCook, O.; Wagner, F.; Groger, M.; Wagner, K.; Scheuerle, A.; Radermacher, P.; Ignatius, A. Exposure to 100% Oxygen Abolishes the Impairment of Fracture Healing after Thoracic Trauma. *PLoS ONE* **2015**, *10*, e0131194. [CrossRef]
21. Gassmann, M.; Fandrey, J.; Bichet, S.; Wartenberg, M.; Marti, H.H.; Bauer, C.; Wenger, R.H.; Acker, H. Oxygen Supply and Oxygen-Dependent Gene Expression in Differentiating Embryonic Stem Cells. *Proc. Natl. Acad. Sci. USA* **1996**, *93*, 2867–2872. [CrossRef]
22. Iida, K.; Takeda-Kawaguchi, T.; Hada, M.; Yuriguchi, M.; Aoki, H.; Tamaoki, N.; Hatakeyama, D.; Kunisada, T.; Shibata, T.; Tezuka, K. Hypoxia-Enhanced Derivation of iPSCs from Human Dental Pulp Cells. *J. Dent. Res.* **2013**, *92*, 905–910. [CrossRef]
23. Kurosawa, H.; Kimura, M.; Noda, T.; Amano, Y. Effect of Oxygen on in Vitro Differentiation of Mouse Embryonic Stem Cells. *J. Biosci. Bioeng.* **2006**, *101*, 26–30. [CrossRef] [PubMed]
24. Ikeda, K.; Nagata, S.; Okitsu, T.; Takeuchi, S. Cell Fiber-Based Three-Dimensional Culture System for Highly Efficient Expansion of Human Induced Pluripotent Stem Cells. *Sci. Rep.* **2017**, *7*, 2850. [CrossRef] [PubMed]
25. Werle, S.B.; Chagastelles, P.; Pranke, P.; Casagrande, L. The Effects of Hypoxia on in Vitro Culture of Dental-Derived Stem Cells. *Arch. Oral Biol.* **2016**, *68*, 13–20. [CrossRef] [PubMed]
26. Zhou, Y.H.; Fan, W.; Xiao, Y. The Effect of Hypoxia on the Stemness and Differentiation Capacity of PDLC and DPC. *Biomed. Res. Int.* **2014**, *2014*, 890675. [CrossRef]
27. Yoshida, Y.; Takahashi, K.; Okita, K.; Ichisaka, T.; Yamanaka, S. Hypoxia Enhances the Generation of Induced Pluripotent Stem Cells. *Cell Stem Cell* **2009**, *5*, 237–241. [CrossRef]
28. Hakim, F.; Kaitsuka, T.; Raeed, J.M.; Wei, F.Y.; Shiraki, N.; Akagi, T.; Yokota, T.; Kume, S.; Tomizawa, K. High Oxygen Condition Facilitates the Differentiation of Mouse and Human Pluripotent Stem Cells into Pancreatic Progenitors and Insulin-Producing Cells. *J. Biol. Chem.* **2014**, *289*, 9623–9638. [CrossRef]
29. An, S.Y.; Heo, J.S. Low Oxygen Tension Modulates the Osteogenic Differentiation of Mouse Embryonic Stem Cells. *Tissue Cell* **2018**, *52*, 9–16. [CrossRef]
30. Sugimoto, K.; Matsuura, T.; Nakazono, A.; Igawa, K.; Yamada, S.; Hayashi, Y. Effects of Hypoxia Inducible Factors on Pluripotency in Human IPS Cells. *Microsc. Res. Tech.* **2018**, *81*, 749–754. [CrossRef]
31. Medley, T.L.; Furtado, M.; Lam, N.T.; Idriji, R.; Williams, D.; Verma, P.J.; Costa, M.; Kaye, D.M. Effect of Oxygen on Cardiac Differentiation in Mouse IPS Cells: Role of Hypoxia Inducible Factor-1 and Wnt/Beta-Catenin Signaling. *PLoS ONE* **2013**, *8*, e80280. [CrossRef]
32. Ezashi, T.; Das, P.; Roberts, R.M. Low O-2 Tensions and the Prevention of Differentiation of HES Cells. *Proc. Natl. Acad. Sci. USA* **2005**, *102*, 4783–4788. [CrossRef]
33. Aranha, A.M.F.; Zhang, Z.C.; Neiva, K.G.; Costa, C.A.S.; Hebling, J.; Nor, J.E. Hypoxia Enhances the Angiogenic Potential of Human Dental Pulp Cells. *J. Endod.* **2010**, *36*, 1633–1637. [CrossRef] [PubMed]
34. Robins, J.C.; Akeno, N.; Mukherjee, A.; Dalal, R.R.; Aronow, B.J.; Koopman, P.; Clemens, T.L. Hypoxia Induces Chondrocyte-Specific Gene Expression in Mesenchymal Cells in Association with Transcriptional Activation of Sox9. *Bone* **2005**, *37*, 313–322. [CrossRef] [PubMed]
35. Compennolle, V.; Brusselmans, K.; Franco, D.; Moorman, A.; Dewerchin, M.; Collen, D.; Carmeliet, P. Cardiac Bifida, Defective Heart Development and Abnormal Neural Crest Migration in Embryos Lacking Hypoxia-Inducible Factor-1 Alpha. *Cardiovasc. Res.* **2003**, *60*, 569–579. [CrossRef] [PubMed]

36. Adelman, D.M.; Gertsenstein, M.; Nagy, A.; Simon, M.C.; Maltepe, E. Placental Cell Fates Are Regulated in Vivo by HIF-Mediated Hypoxia Responses. *Genes Dev.* **2000**, *14*, 3191–3203. [[CrossRef](#)] [[PubMed](#)]
37. Mathieu, J.; Zhou, W.Y.; Xing, Y.L.; Sperber, H.; Ferreccio, A.; Agoston, Z.; Kuppusamy, K.T.; Moon, R.T.; Ruohola-Baker, H. Hypoxia-Inducible Factors Have Distinct and Stage-Specific Roles during Reprogramming of Human Cells to Pluripotency. *Cell Stem Cell* **2014**, *14*, 592–605. [[CrossRef](#)] [[PubMed](#)]
38. Sperber, H.; Mathieu, J.; Wang, Y.L.; Ferreccio, A.; Hesson, J.; Xu, Z.J.; Fischer, K.A.; Devi, A.; Detraux, D.; Gu, H.W.; et al. The Metabolome Regulates the Epigenetic Landscape during Naive-to-Primed Human Embryonic Stem Cell Transition. *Nat. Cell Biol.* **2015**, *17*, 1523–1535. [[CrossRef](#)]
39. Gu, W.; Gaeta, X.; Sahakyan, A.; Chan, A.B.; Hong, C.S.; Kim, R.; Braas, D.; Plath, K.; Lowry, W.E.; Christofk, H.R. Glycolytic Metabolism Plays a Functional Role in Regulating Human Pluripotent Stem Cell State. *Cell Stem Cell* **2016**, *19*, 476–490. [[CrossRef](#)]
40. Rossant, J. Mouse and Human Blastocyst-Derived Stem Cells: Vive Les Differences. *Development* **2015**, *142*, 9–12. [[CrossRef](#)]

Disclaimer/Publisher’s Note: The statements, opinions and data contained in all publications are solely those of the individual author(s) and contributor(s) and not of MDPI and/or the editor(s). MDPI and/or the editor(s) disclaim responsibility for any injury to people or property resulting from any ideas, methods, instructions or products referred to in the content.